

A NOVEL 2-D PROGRAMMABLE PHOTONIC TIME DELAY DEVICE FOR
MM-WAVE SIGNAL PROCESSING APPLICATIONS

X. Steve Yao and Lute Maleki
Jet Propulsion laboratory
California Institute of Technology
4800 Oak Grove Drive, Pasadena, CA 91109
Tel: (818) 393-9031 Fax: (818) 393-6773
E-mail: xsyao@fridge.jpl.nasa.gov

We describe a novel programmable photonic true time delay device that has the properties of low loss, inherent two dimensionality with a packing density exceeding 25 lines/cm², virtually infinite bandwidth, and is easy to manufacture. The delay resolution of the device is on the order of a femtosecond (one micron in space) and the total delay exceeds 1 nanosecond (30 cm in space).

For airborne and space-based phased array antennas¹ operating at mm-wave frequencies (20 GHz and above), two dimensional beam forming networks of high packing density, low loss, light weight, remoting capability, and immunity to electromagnetic interference are required. Photonic technology is naturally suited for such applications.²⁻⁵ However, none of the proposed photonic beam forming networks to date meet all of the requirements specific to the mm-wave phased arrays, particularly the requirements of high operation frequency, high packing density, and fine delay resolution (the minimum step of delay change). The delay resolution is important and must be fine enough (much less than the wavelength of the signal) to ensure that the angular resolution of the beam scanning is sufficient.

The true-time-delay beam forming networks²⁻⁴ based on acousto-optic modulators are limited by low operation frequency (below 10 GHz) and narrow bandwidth (below 100 MHz). The path-switching time delay devices based on guided wave optics⁶⁻⁸ are complicated and are characterized by high loss, high cost, poor delay resolution, and one-dimensional geometry. The free-space path-switching time delay device proposed by Riza^{9,10} is 2-D with high packing density, and operates at high frequency with sufficient total delay. However, the optical path delay resolution of the device is limited by the size of the vertical dimension of the 2-D delay array and is inadequate for signals with a wavelength of only few millimeters.

In this paper we describe a novel photonic true time delay device that is suitable for mm-wave phased arrays. This programmable device is inherently two dimensional, and has the properties of high packing density, low loss, easy fabrication, and virtually infinite bandwidth. The delay resolution of the device is sufficiently fine for accurate beam steering, and the total delay is

adequately large to cover desired scanning angles. This device can also be simplified to a phase-shifter beam-former for phased arrays of narrow bandwidth, where true time delay is not necessary. The same device is also suitable for photonic mm-wave transversal (adaptive) filters^{11,12}

Figure 1a depicts the proposed index switched true time delay device. The delay unit consists of birefringent crystal segments. Each segment is cut along the principal axes of the crystal with the light beam propagating along the X (or Y axis). The light beam is polarized either in the Z direction or in the Y (or X) direction (the two principal directions of the crystal). The Y (or X) polarized beam experiences a refractive index of n_o and the Z polarized beam experiences a refractive index of n_e . A polarization rotator is sandwiched between each pair of segments to change the beam's polarization states by 90 degrees, either from Y (or X) to Z or from Z to Y (or X). The polarization rotator can be a liquid crystal, a magneto-optic or an electro-optic element. It is evident from Fig. 1a that the time delay of the beam can easily be altered by changing the beam's polarization in each segment. We call this method index-switching technique.

To minimize¹³ the number of polarization rotators in the device, the lengths of the crystal segments increase successively by a factor of 2, as shown in Fig. 1a. The relative optical path delay Δl between the two polarization states in the smallest segment of length l (the least significant bit) is

$$\Delta l = (n_e - n_o)l. \quad (1)$$

Let M be the total number of crystal segments (or bits), then the maximum value of the optical path delay generated is:

$$\Delta l_{\max} = (2^0 + 2^1 + 2^2 + \dots + 2^{M-1})\Delta l = (2^M - 1)\Delta l \quad (2)$$

By properly adjusting the polarization state of the light beam in each segment, any time delay in the range from $\Delta l/c$ to $\Delta l_{\max}/c$ can be obtained with a resolution (or delay increment) of $\Delta l/c$. Because the length of each crystal segment can be tightly controlled, the accuracy of the device can be very high.

Table I lists the refractive indices and the corresponding delay rates (time delay per unit length) of potential birefringent materials for fabricating the proposed delay lines. Note that different crystals may be used together to construct a delay line: a crystal with small birefringence can be used to make segments of small delays (less significant bits) and a crystal with large birefringence can be used to make segments of large delays (more significant bits).

The maximum delay ΔT_{\max} required of a beam forming network of a phased array antenna with $N \times N$ elements is¹

$$\Delta l_{\max} = (N - 1)d_{\max} \sin|\theta_{\max}| = \frac{(N - 1)\lambda \cdot \sin|\theta_{\max}|}{(1 + \sin|\theta_{\max}|)} \quad (3)$$

where θ_{\max} is the maximum beam scanning angle, λ is the wavelength of the carrier (microwave) signal of the phased array, and $d_{\max} \equiv A/(1 + \sin|\theta_{\max}|)$ is the maximum array spacing¹ allowed before higher order diffraction degrade the antenna gain.

To achieve an angular beam scanning resolution of $\Delta\theta$, the delay resolution or the minimum path delay between the two adjacent elements Δl is required to be

$$\Delta l = \frac{\lambda \cos\theta_{\max} \Delta\theta}{(1 + \sin|\theta_{\max}|)} \quad (4)$$

Table II lists the values of required maximum delay ΔL_{\max} and delay resolution Δl for a phased array with $\lambda = 0.75$ cm (40 GHz), $N = 64$, and $\Delta\theta = 1^\circ$. The corresponding crystal lengths for the maximum and the minimum delays are also listed. For example, for the case of $\theta_{\max} = 30^\circ$, LiNbO₃ crystal of length 0.87 mm can be used to make the segment of the smallest delay of 76,5 pm and the Rutile crystal of the total length of about 55 cm can be used to make other larger delay segments that have a total delay of 15.75 cm. In the table, the number of bits M is calculated using $M = \log_2(1 + \Delta L_{\max}/\Delta l)$.

The same concept can also be used to make phase shifters for phased array antennas with narrow bandwidth where true time delay is not necessary. For example, an 8 GHz (X-band) carrier has a wavelength of 3.75 cm. To obtain a total phase shift of 2π for such a carrier, a total length of only 13 cm of Rutile crystal per channel is required. For a Ka band carrier of wavelength of 0.75 cm (40 GHz), only 2.6 cm Rutile crystal per channel is required.

It should be noted that Rutile has excellent optical and physical properties:¹⁴ it is transparent to light from 500 nm to 5 μ m and its birefringence ($n_e - n_o$) remains almost unchanged from 430 nm to 4 μ m. It has a density of 4.26 g/cm³, a melting point of 2,093 °K, and a solubility in water less than 0.001,

Several delay lines of the design described above can be densely packed in 2 dimensions to form a compact beam forming network, as shown in Fig. 1b. The spatial light modulators are used to control the polarization in each segment of each channel. For 2 mm channel spacing, the packing density of the device is 25/cm². Such a channel spacing is easily attainable in practice, considering that a 1.4 mm diameter Gaussian beam with 1 μ m wavelength has a Rayleigh range of 1.54 meters.

To reduce the cost and to extend the delay range, the index-changing delay elements may be cascaded with a free-space path-switching delay device of Riza,⁹ as shown in Fig. 2. The birefringent crystal segments are used for the less significant bits of high delay resolution and the path switching concept is used for the more significant bits of large delays. This cascaded construction combines the advantages of both techniques and avoids their shortcomings. The total length of the crystal segments per channel is now reduced to few centimeters. Note that the architecture of the path-switching time delay device depicted here is dramatically different from those previously published and is much more compact and simple to fabricate.

Instead of using many segments, the index-switching time delay unit may also be constructed using a single slab of a crystal, as shown in Fig. 3. Such a unit consists of a slab of a birefringent crystal, a layer of polarization rotation cells (which may be individually and independently controlled), and two rows of corner reflectors. The slab is cut along the principal axes of the crystal and light beam propagates along the X (or Y axis). The beam is polarized either in the Z direction or in the Y (or X) direction (two principal directions of the crystal). Similar to the linear construction described in Fig. 1, here the polarization state of the light beam can also be easily switched between Y and Z directions by the 90° polarization rotation cells and the beam will experience n_o and n_e accordingly. In this configuration the height of the crystal determines the smallest delay (delay resolution) and the total number of paths determines the maximum delay. The spacing between the polarization rotation cells increases successively by a factor of 2 to make the delay line binary, as in Fig. 1. As shown in Fig. 3, many crystal slabs may be stacked together to construct a one dimensional delay array. Finally, to obtain

even finer delay tuning, electrodes can be attached across each crystal slab to apply an electrical field and change the refractive index of the crystal via the electro-optic (or Pockel's) effect of the birefringent crystals, as shown Fig. 3. Compared with the linear construction of Fig. 1, the zig-zag construction uses less crystal. However, it is inherently one dimensional and thus has a lower packing density than that of the linear construction.

In summary, we have described a novel programmable photonic true time delay device that has the properties of high packing density, low loss, easy fabrication, and virtually infinite bandwidth. The device is inherently two dimensional and has a packing density exceeding 25 lines/cm². The delay resolution of the device is on the order of a femtosecond (one micron in space) and its total delay exceeds 1 nanosecond. The delay accuracy achievable is high, and is only limited by the length accuracy of each crystal segment. The device can also be digitally programmed with low switching power (microwatts per switch or per bit). Such a device is ideal for a beam forming network of a phased array operating at Ka band (40 GHz) and higher frequencies and for millimeter wave transversal filters.

This study represents the results of research carried out at the Jet Propulsion Laboratory, California Institute of Technology, under a contract sponsored by NASA. We thank G. Lutes for many helpful discussions and suggestions.

REFERENCES:

1. R. Tang and R. W. Burns, "Phased arrays" in *Antenna Engineering Handbook*, R. C. Johnson Ed, 3rd ed. New York: McGraw-Hill, 1992, ch. 20.
2. E. Toughlian and H. Zmuda, "A photonic variable RF delay line for phased array antennas," *J. of Lightwave Technology*, vol. 8, pp. 1824-1828 (1990).
3. D. D. Dolfi, F. Michel-Gabriel, S. Bann, and J. P. Huignard, "Two-dimensional optical architecture for time-delay beam forming in a phased-array antenna," *Opt. Lett.*, vol. 16, pp. 255-257 (1991),
4. N. A. Riza, "An acoustooptic phased array antenna beamformer with independent phase and carrier control using single sideband signals," *IEEE Photonics Technology Letters*, vol. 4, pp. 177-179 (1992).
5. P. Herczfeld and A. Daryoush, "Fiber optic feed network for large aperture phased array antennas," *Microwave Journal*, August 1987, pp. 160-166.
6. R. A. Soref, "Programmable time delay device," *Appl. Opt.*, vol. 23, pp. 3736-3737 (1984).
7. W. Ng, A. Walston, G. Tangonan, J. J. Lee, I. Newberg, and N. Bernstein, "The first demonstration of an optically steered microwave phased array antenna using true-time-delay," *J. of Lightwave Technology*, vol. 9, pp. 1124-1131 (1991).
8. C. T. Sullivan, S. D. Mukherjee, M. K. Hibbs-Brenner, and A. Gopinath, "Switched time delay elements based on AlGaAs/GaAs optical waveguide technology at 1.32 μm for optically controlled phased array antennas," *SPLE Proceedings Vol. 1703* (1992), pp. 264-271.
9. N. A. Riza, "Transmit/receive time-delay beam-forming optical architecture for phased array antennas," *Appl. Opt.*, vol. 30, pp. 4594-4595 (1991).
- 10.11. R. Fetterman, Y. Chang, D. C. Scott, and D. V. Plant, "Optically controlled phased array radar receiver using true-time-delay," presented at

4th Annual ARPA Symposium on photonics systems for antenna applications, Monterey, CA, January 1994.

11. D. Norton, S. Johns, and R. Soref, "Tunable wideband microwave transversal filter using high dispersive fiber delay lines," Proceedings of the 4th biennial Department of Defense fiber optics and Photonics Conference, McLean, Virginia, 1994, pp297-301.

12. B. Moslehi, K. Chau, and J. Goodman, "Fiber-optic signal processors with optical gain and reconfigurable weights," *ibid*, pp303-309.

13. A. I'. Goutzoulis and D. K. Davies, "Hardware-compressive 2-D fiber optic delay line architecture for time steering of phased array antennas," *Appl. Opt.* vol. 29, pp. 5353-5359 (1990).

14. A. J. Moses, "Optical Materials Properties," in *Handbook of Electronic Materials, vol.1*, New York: IFI/Plenum, 1971, p96.

15. E. Hecht and A. Zajac, *Optics*, Reading, Massachusetts: Addison-Wesley, 1974, ch.8, pp219-271.

16. A. Yariv and P. Yeh, *Optical waves in Crystals*, New York: John Wiley & Sons, 1984, ch. 7, pp230-234.

FIGURE CAPTIONS

Fig. 1

a) Illustration of an index-switched true time delay device. Optical path delay of the modulated light beam is varied by rotating the polarization of the beam so that it experiences either n_o or n_e of the refractive index in each crystal segment, To compress the number of polarization rotators, binary delay variation is preferred and depicted. b) Many delay lines are densely packed to form a 2-D time delay beam forming device for a phased array antenna.

Fig. 2

Cascading an index-switched delay unit with a path-switched delay unit. The total delay is 8 bits. The first six bits have smaller delay increments and use index-switched technique to construct. The last two bits have large delay increments and therefore use path-switching technique.

Fig. 3

The zig-zag construction of the index-switched delay device. Many such delays (three are shown) can be stacked together to form a 1-D array. Electrodes can be placed on each slabs so that electric field can be applied to the crystal slabs for fine tuning the delay via electrooptic effect of the crystal,

TABLE CAPTIONS

Table I

The potential birefringent materials for the index-switched delay device and their birefringence. Data for materials marked with "*" are from reference 15 and the data for other crystals are from reference 16, The data for the I'M fiber is from 3M Corporation's data sheet.

Table 11

The required maximum delay and delay resolution for a phased array of $N \times N$ elements, an operation frequency of 40 GHz (0.75 cm), and a beam scanning angle resolution of 1° . The requirements of corresponding crystal length and total number of bits are also listed.

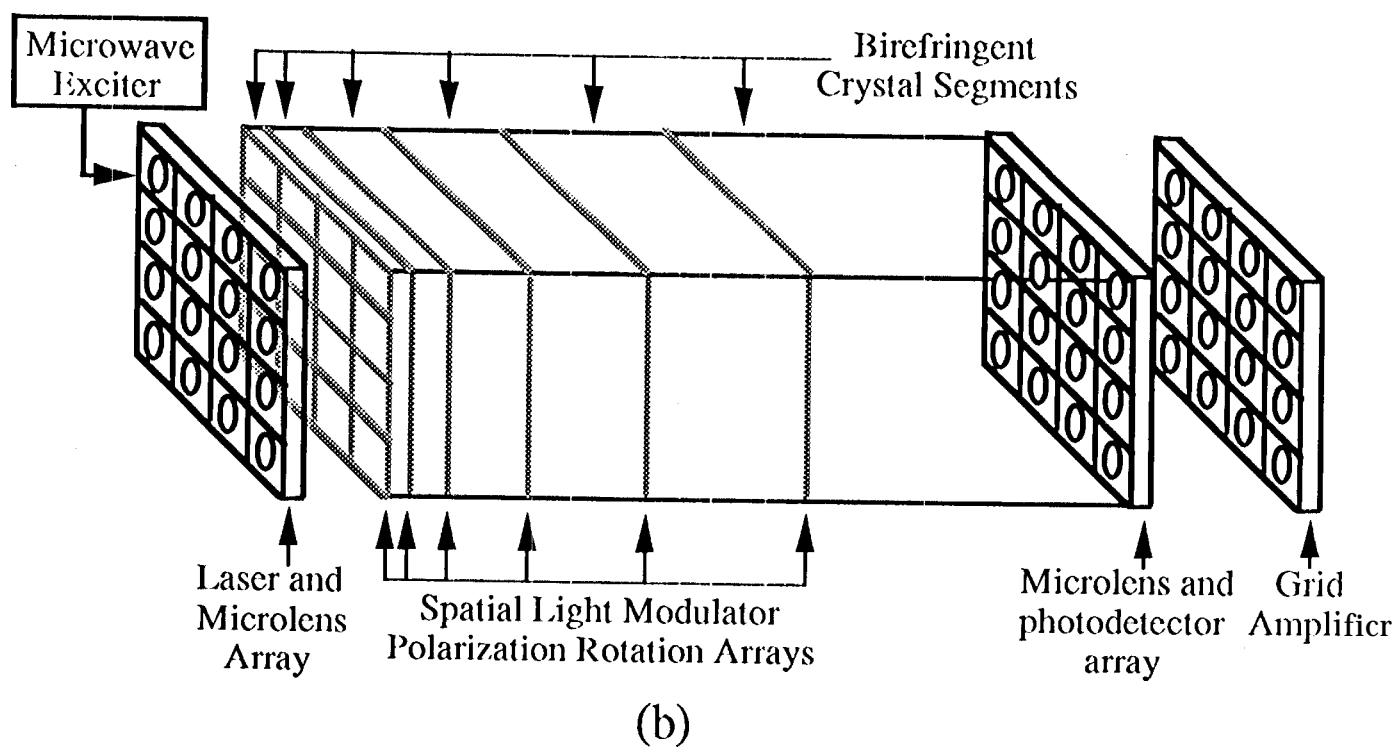
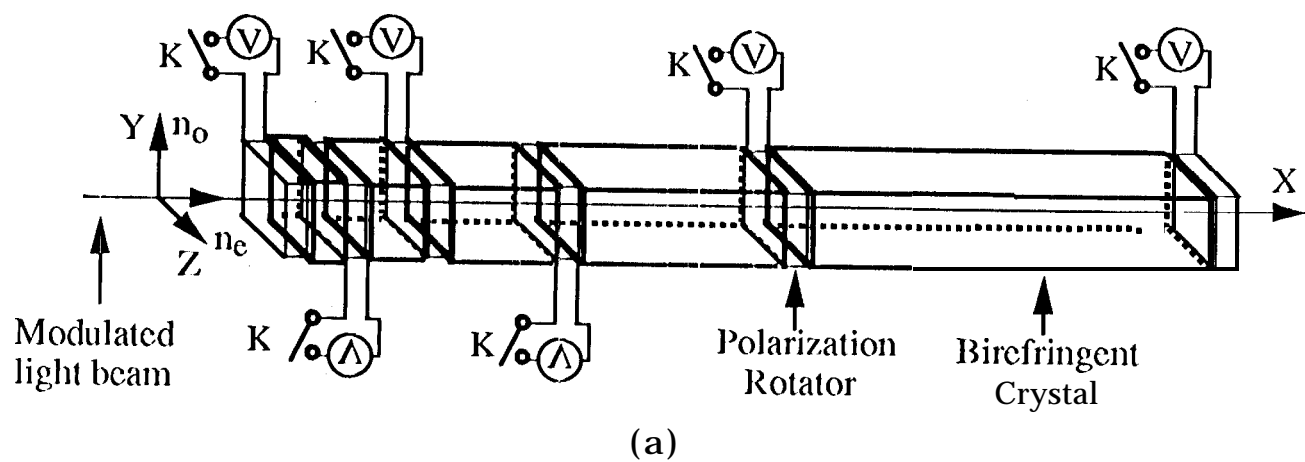


Fig. 1

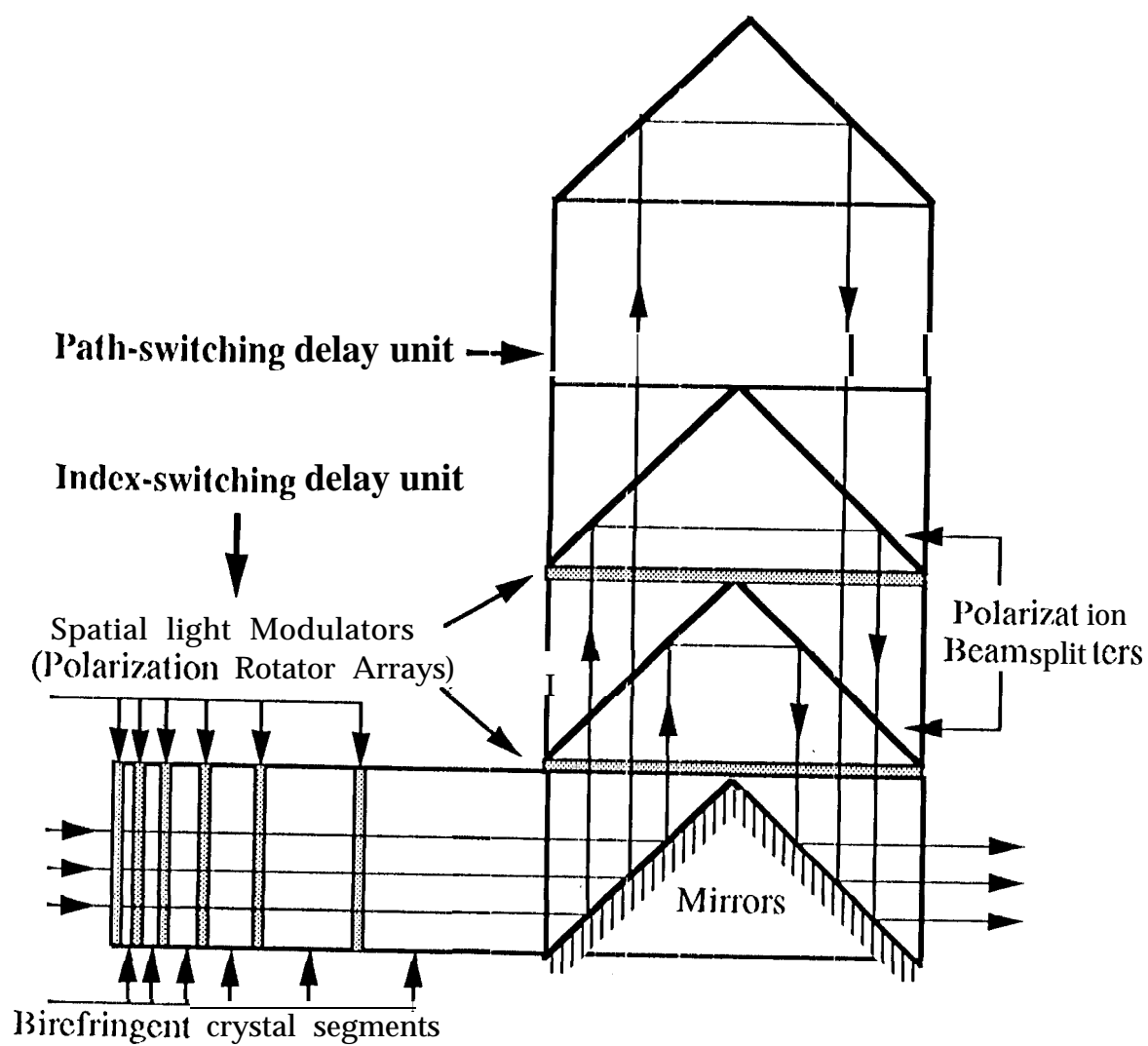


Fig. 2

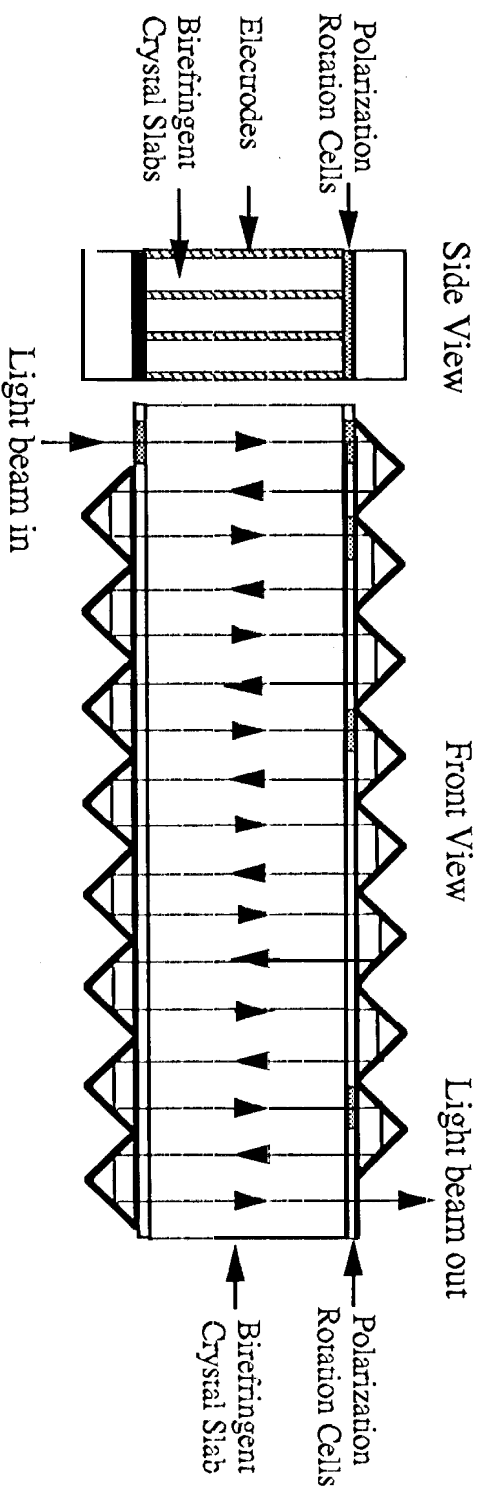


Fig. 3

Table I

	n_e	n_o	$n_e - n_o$	$\Delta\tau/\text{mm}$
Rutile (TiO_3)* ($\lambda = 589.3 \text{ nm}$)	2.903	2.616	0.287	0.96 ps/mm
Ag_3AsS_3 ($\lambda = 633 \text{ nm}$)	2.739	3.019	0.28	0.93 ps/mm
Sodium Nitrate* ($\lambda = 589.3 \text{ nm}$)	1.3369	1.58s4	-0.2485	0.83 ps/mm
Calcite* ($\lambda = 589.3 \text{ nm}$)	1.4864	1.6584	-0.172	0.57 ps /mm
LiNbO_3 ($\lambda = 633 \text{ nm}$)	2.2	2.286	-0.086	0.29 ps /mm
LiTaO_3 ($\lambda = 633 \text{ nm}$)	2.18	2.176	0.04	0.13 ps /mm
Quartz* ($\lambda = 589.3 \text{ nm}$)	1.5534	1.5443	0.0091	0.03 ps /mm
PM Fiber ($\lambda = 1300 \text{ nm}$)			$\sim 6 \times 10^{-4}$	$\sim 2 \text{ fs /mm}$

Table II

	$\theta_{\max} = 5^\circ$	$\theta_{\max} = 10^\circ$	$\theta_{\max} = 30^\circ$	$\theta_{\max} = 60^\circ$
ΔL_{\max}	3.78 cm or 5.04 λ	7 cm or 933 λ	15.75 cm or 21 λ	21.93 cm or 29.24 λ
L_{\max} (l<utile)	13.48 cm	24.4 cm	55 cm	76.4 cm
Al	0.12 mm	0.11 mm	0.0756 mm	0.035 mm
¹ (LiNbO ₃)	1.4 mm	1.3 mm	0.87 mm	0.41 mm
M No. of bits	7	8	11	12